Evaluation and extension of the two-site, two-step model for binding and activation of the chemokine receptor CCR1

Julie Sanchez[‡,§], **Zil e Huma** [‡,§], **J. Robert Lane**[#,§], **Xuyu Liu**[¶], **Jessica L. Bridgford**[‡,§], **Richard J. Payne**[¶], **Meritxell Canals**[§,#,1], and **Martin J. Stone**[‡,1]

From the [‡]Infection and Immunity Program, Monash Biomedicine Discovery Institute, and Department of Biochemistry and Molecular Biology, Monash University, Clayton, VIC 3800, Australia, [§]Drug Discovery Biology, Monash Institute of Pharmaceutical Sciences, Monash University, Parkville, VIC 3052, Australia, [¶]School of Chemistry, The University of Sydney, NSW 2006, Australia, and the Centre for Membrane Proteins and Receptors, Nottingham University, Nottingham, United Kingdom.

Running title: *Extension of two-site, two-step model at CCR1*

[1]To whom correspondence should be addressed: (MJS) Department of Biochemistry and Molecular Biology, Monash University, Clayton, VIC 3800, Australia. Tel. +61 3 9902 9246; E-mail: martin.stone@monash.edu; (MC) Centre for Membrane Proteins and Receptors, Nottingham University, Nottingham, NG7 2UH, United Kingdom; E-mail: meritxell.canals@nottingham.ac.uk.

Keywords: Chemokine, chemokine receptor, CCR1, binding, receptor activation, three-step model, cytokine, innate immunity.

ABSTRACT

Interactions between secreted immune proteins called chemokines and their cognate G protein–coupled receptors regulate the trafficking of leukocytes in inflammatory responses. The two-site, two-step model describes these interactions. It involves initial binding of the chemokine N-loop/β3 region to the receptor's N-terminal region and subsequent insertion of the chemokine N-terminal region into the transmembrane helical bundle of the receptor concurrent with receptor activation. Here we test aspects of this model with CC motif chemokine receptor 1 (CCR1) and several chemokine ligands. First, we compared the chemokine-binding affinities of CCR1 with those of peptides corresponding to the CCR1 N-terminal region. Relatively low affinities of the peptides and poor correlations between CCR1 and peptide affinities indicated that other regions of the receptor may contribute to binding affinity. Second, we evaluated the contributions of the two CCR1-interacting regions of the cognate chemokine ligand CCL7 (formerly monocyte chemoattractant protein-3, MCP-3) using chimeras between CCL7 and the non-cognate ligand CCL2 (formerly MCP-1). The results revealed that the chemokine N-terminal region contributes significantly to binding affinity but that differences in binding affinity do not completely account for differences in receptor activation. On the basis of these observations, we propose an elaboration of the two-site, two-step model— the "three-step" model—in which initial interactions of the first site result in low-affinity, non-specific binding; rate-limiting engagement of the second site enables high-affinity, specific binding; and subsequent conformational rearrangement gives rise to receptor activation.

The interactions between chemokines and chemokine receptors regulate the trafficking of leukocytes, a key feature of inflammatory responses (1,2). Chemokines are small proteins secreted by various tissues as part of normal immune surveillance or in response to tissue injury or infection. Chemokines bind to and activate chemokine receptors, which are G protein-coupled receptors (GPCRs) expressed in leukocyte cell membranes. This initiates intracellular signal transduction leading to changes in leukocyte morphology and adhesion and ultimately giving rise to accumulation of leukocytes in the affected tissues. Due to the importance of this process in numerous inflammatory diseases, there is substantial interest in understanding the detailed molecular mechanisms of chemokine-receptor interactions and signaling.

CCR1, a member of the CC chemokine receptor subfamily, is expressed on the surfaces

of monocytes, natural killer cells and immature myeloid cells (3,4). At least nine CC chemokines are reported to be cognate agonists of CCR1 (5). Activation of CCR1 has been implicated in the pathology of rheumatoid arthritis (6), multiple sclerosis (7), multiple myeloma (8,9), transplant rejection (10), diabetes (11), osteopenia (12) and progressive kidney disease (13). As with other chemokine receptors, clinical trials targeting CCR1 with anti-inflammatory drug candidates have not been successful to date but CCR1 is still considered a valid therapeutic target (14).

Numerous studies have investigated the molecular determinants of chemokine receptor binding and activation. Early studies identified two distinct regions of chemokines that interact with distinct regions of their receptors (15). The chemokine "N-loop" and nearby β3 region, together defined as chemokine site 1 (CS1), were found to bind to peptides corresponding to the flexible N-terminal regions of chemokine receptors, defined as chemokine receptor site 1 (CRS1). In addition, the N-terminal region of the chemokine (CS2) was found to be critical for receptor activation, so it was proposed that this region interacts with a second site on the receptor (CRS2), later found to be predominantly located within the transmembrane (TM) bundle of the receptor, with some contributions from extracellular loops (16,17).

Based on these early observations, Crump et al. proposed the two-site, two-step model as a general paradigm for chemokine-receptor interactions (15). According to this model, CS1-CRS1 form first and contribute to binding without receptor activation. Subsequently, engagement of CS2 with CRS2 induces a conformational change and receptor activation. This model remains consistent with much of the available functional and structural data, including a study of chimeric receptors formed by exchanging regions of CCR1 and the related receptor CCR3 (18). However, a number of observations point to possible deficiencies in this simple model. In particular, mutations in CS2 can influence receptor binding affinity, suggesting that binding and activation are not simply partitioned between the two structural sites (19,20). Similarly, different chemokine agonists of the same receptor can selectively interact with different regions of a receptor (21) or can "bias" a shared receptor towards activation of different signaling pathways (22,23), suggesting distinct activated conformations of the receptor. Moreover, recent structural data and models indicate that residues outside of the two primary sites may also make important contributions to binding and receptor activation (16,24). As discussed in a detailed review by Volkman and colleagues (25), there is a need to consider possible elaborations of the two-site, two-step model.

In the study described herein, we have taken two approaches to evaluate specific aspects of the two-site, two-step model for CCR1 and several of its chemokine ligands. First, we have compared the chemokine binding affinities of CCR1 to those of peptides corresponding to the N-terminus (CRS1) of CCR1, allowing us to evaluate the contributions of CRS1 to both affinity and selectivity of chemokine binding. Second, we have compared CCR1 binding and activation by chimeric chemokines derived from a high affinity cognate chemokine and a low affinity chemokine, enabling the contributions of CS1 and CS2 to be evaluated. The data indicated that CS2-CRS2 interactions contribute significantly to binding affinity but that differences in binding affinity do not completely account for differences in receptor activation. These results prompted us to propose an extension of the two-site, two-step model (the "three-step" model) in which: initial CS1-CRS1 interactions result in low affinity, non-specific binding; rate-limiting engagement of CS2 with CRS2 enables high affinity, specific binding; and subsequent conformational rearrangement gives rise to receptor activation.

RESULTS

Chemokine Binding to N-terminal CCR1 Peptides – The N-terminal regions of chemokine receptors are thought to be flexible and essentially unstructured. Therefore, peptides corresponding to this region are often used as simplified models of CRS1 (26-38). If the site 1 interactions make a major contribution to the binding interactions, one would anticipate that the binding free energy of such N-terminal peptides for chemokines would be a substantial proportion of the binding free energy of intact receptors for the same chemokines. Moreover, it would be expected that the binding free energies (or affinities) of several chemokines would correlate for the N-terminal peptides and the intact receptors. To test these hypotheses, we measured the binding affinities of peptides with the N-terminal sequence of CCR1 and of intact CCR1 expressed on mammalian cells to each of four cognate chemokine ligands (CCL15/HCC-2, CCL5/RANTES, CCL7/MCP-3 and

CCL8/MCP-2) as well as two chemokines that are not usually considered cognate ligands of CCR1 (CCL2/MCP-1 and CCL26/eotaxin-3).

The N-terminus of CCR1 contains two predicted sites of tyrosine sulfation (Tyr-10 and Tyr-18) (39), although it has not been determined whether these sites are actually sulfated in CCR1; sulfation could also be incomplete or vary for different cell types. Considering that sulfation in the N-terminal regions of chemokine receptors can alter both the affinity and selectivity of chemokine binding (40), we prepared a set of peptides with all four possible combinations of sulfation at these two sites (Fig 1A) and used an established competitive fluorescence anisotropy binding assay (41) to measure their binding affinities for the six chemokines (Fig 1B-G, Table 1; Fig S1, Table S1). Affinities ranged from ~40 nM to ~24 μM and were well correlated between different peptides (r^2 = 0.70 to 0.98; Fig S2), indicating that sulfation has only a small influence on the selectivity of the CCR1 N-terminal peptide for chemokine ligands.

Contribution of Site 1 Interactions to CCR1 Binding Affinity and Selectivity – We assessed the affinities of chemokines for CCR1 expressed in Flp-In T-REx human embryonic kidney (HEK) 293 cells using a radioligand displacement assay (Fig 2A,B and Table 2). The results are consistent with previous reports of chemokine-CCR1 binding affinities (42-44). Although the sulfation status of CCR1 is unknown, we also determined the affinities of the same chemokines for CCR1 derived from cells treated with 30 mM chlorate, which blocks tyrosine sulfation. Effective prevention of sulfation by 30 mM chlorate was verified using ELISA for two chemokine receptors N-terminally tagged with both FLAG, for which antibody detection is blocked by sulfation (45), and cMyc, which cannot be sulfated (Fig S3). We found that the chemokine affinities were not significantly different for CCR1 derived from untreated cells and cells treated with 30 mM chlorate (Fig 2A,B and Table 2). This indicates that either CCR1 is not sulfated in these cells or sulfation has no effect on chemokine affinity.

As expected, the affinities of chemokines were higher for CCR1 than for the N-terminal peptides. For most chemokines, the intact receptor bound with affinities in the range 0.07-60 nM, whereas the peptides bound about 1000-fold less tightly. These data indicate that, in general, approximately two-thirds of the receptor binding free energy can be attributed to the interactions at site 1. The only exception was CCL26, which bound to the peptides (K_d ~0.1-4 μM) but for which CCR1 binding could not be detected at concentrations up to 0.1 μM. CCL26 is not a cognate ligand for CCR1. It is possible that this chemokine binds to CRS1 of CCR1 with an affinity comparable to its affinity for the non-sulfated N-terminal peptide but without any additional interactions with CRS2.

To assess the contribution of the receptor N-terminus to the selectivity of receptor binding, sulfopeptide binding affinities (pK_d) were correlated with intact receptor binding affinities (pIC_{50}). In all cases, the correlations were very poor (r^2 = 0.02 to 0.16; Fig 3). One possible explanation for such poor correlations is that the interactions of the chemokines at CRS1 may differ substantially for the intact receptor and the receptor derived peptides, or be substantially influenced by local structural constraints in the intact receptor. An alternative explanation is that CRS1 interactions alone do not play a dominant role in defining the chemokine binding selectivity and additional interactions of CRS2 also contribute.

Evaluation of Site 1 and Site 2 interactions using Chemokine Chimeras – The chemokine CCL7 is a potent cognate ligand for CCR1 (42), whereas the closely related chemokine CCL2 has much lower potency and affinity for CCR1 and is not generally considered a cognate ligand for this receptor. Therefore, these two chemokines present an opportunity to dissect the contributions of different structural elements of chemokines to CCR1 binding and activation. For this purpose we used two sets of chimeric chemokines based on CCL2 and CCL7 (Fig 4; includes nomenclature); we used the obligate monomeric mutant CCL2(P8A) to ensure consistency with the naturally monomeric CCL7 (46,47). In each chimera, one of three key regions for receptor recognition (N-terminus, N-loop and β3 region) was substituted for the corresponding region from the other chemokine or all three regions were substituted together. To avoid disrupting the folded structures of the chemokines, hydrophobic core residues were excluded from being replaced. As described in a previous study of their interactions with CCR2, all of the chimeras are well folded (20).

For the parental chemokines and each chimera, we evaluated binding to CCR1 using the radioligand displacement assay. In addition, we measured signaling via CCR1 expressed on Flp-

In T-REx 293 cells using proximal measurements of receptor activation (recruitment of β-Arrestin 2; βArr and G protein activation) and two downstream, amplified signals: inhibition of cAMP production; and phosphorylation of extracellular signal-regulated kinases 1 and 2 (ERK1/2).

As expected, CCL7 bound with significantly higher affinity than CCL2 to CCR1 (pIC_{50} values of 9.0 ± 0.1 and 7.2 ± 0.2, respectively, $p < 0.0001$; Fig 5A, Table 3), exhibited a higher maximal effect (E_{max}) in the proximal βArr assay ($p = 0.0046$; Fig 5B, Table 3) and displayed higher potency (pEC_{50}) in the three amplified signaling assays ($p \leq 0.0001$, Fig 5C-E, Table 3). These data indicate that, relative to CCL7, CCL2 is a partial agonist of CCR1.

The chimera in which all three regions of CCL7 were replaced by those of CCL2 (CCL7-222) had CCR1 binding affinity very similar to that of CCL2, whereas the inverse chimera (CCL2-777) had CCR1 binding affinity very similar to that of CCL7 (Fig 5A-E, Table 3). In addition, the chimera CCL7-222 displayed the partial agonist activity of CCL2 whereas CCL2-777 displays the full agonism of CCL7. This trend was observed in all four measurements of receptor activation. These results verify that the three swapped regions are the primary regions of these two chemokines responsible for their differences in CCR1 binding and activation.

Contributions of Chemokine N-loop and β3 Regions to CCR1 Binding and Activation – According to the two-site model the N-loop and β3 regions of chemokines, which together constitute CS1, are expected to contribute to receptor binding affinity. We found that replacement of the β3 region of CCL2 with that of CCL7 (chimera CCL2-227) or the inverse replacement (chimera CCL7-772) had little influence on CCR1 binding affinity or on the signaling profiles of these chemokines (Fig 6A-E, Table 3). On the other hand, replacement of the N-loop of CCL2 with that of CCL7 (chimera CCL2-272) increased the CCR1 binding affinity to be the same as that of wild type CCL7, whereas replacement of the N-loop of CCL7 with that of CCL2 (chimera CCL7-727) decreased the binding affinity to be similar to that of CCL2 (Fig 7A, Table 3). Interestingly, these two chimeras displayed signaling profiles in all four assays that were intermediate between the full agonism of CCL7 and the partial agonism of CCL2 (Fig 7B-E, Table 3). This indicates that the replacement of the N-loop alone is not sufficient to completely overcome the differences in receptor activation despite conferring the affinity of the donor chemokine.

Contribution of Chemokine N-terminus to CCR1 Binding and Activation – In the two-site two-step model, the chemokine N-terminus (CS2) is not involved in initial binding interactions but engages with the receptor TM region (CRS2) in the second step to activate the receptor. However, we observed that swapping the N-terminus gives chimeras (CCL2-722 and CCL7-277) that display an intermediate CCR1 affinity between those of the parental chemokines (Fig 8A, Table 3). This indicates that the N-terminus does contribute to binding affinity. The activation profiles of these chimeras were also intermediate between those of the full and partial agonist activities of the parental chemokines (Fig 8B-D, Table 3). This suggests that the N-terminal region of the chemokines contributes not only to activation of the receptor but is also a determinant of high affinity binding.

DISCUSSION

The two-site, two-step model suggests that most of the binding energy is provided by site 1 interactions. In this study, we observed that peptides derived from the N-terminal region (CRS1) of CCR1 bind to cognate chemokines with affinities ranging from ~40 nM to ~24 μM. In comparison, CCR1 on cell membranes bound to the same chemokines with affinities of ~70 pM to ~2 nM. It is not straightforward to deduce the relative free energies of binding interactions at each site because both receptor binding and peptide binding is expected to be accompanied by loss of overall rotational and translational entropy. Moreover, the peptides used here (and those used in other studies) may differ substantially in their structural ensembles and constraints from the N-terminal region of the intact receptor. Nevertheless, under the assumption that the affinities of the peptides are a reasonable approximation of the contributions of site 1 to binding affinity, our data indicate that the site 1 interactions contribute at least ~50% of the total free energy for chemokine-receptor binding if the receptor is not sulfated and ~60-90% (depending on the chemokine) of the total binding free energy if the receptor is sulfated at both possible sites. This conclusion can be taken as supporting the importance of site 1 for binding. However, it also highlights that subsequent interactions may also

contribute a substantial proportion of binding free energy.

Two aspects of the peptide binding data point to possible deficiencies in the two-site, two-step model. First, we found that the N-terminal peptides bound to two non-cognate chemokines of CCR1 (CCL2 and CCL26) with affinities comparable to those of cognate ligands; as expected, these chemokines bound more weakly than the cognate ligands to CCR1 on cell membranes. Second, there was no correlation between peptide affinities and receptor affinities (Fig 3), indicating that site 1 interactions may not play a dominant role in controlling the chemokine selectivity of the receptor. These observations suggest that site 1 may be the initial site of chemokine binding for both cognate and non-cognate ligands, but that additional interactions are required for selective recognition of cognate ligands.

The CCR1 binding affinities of the CCL7/CCL2 chimeras support the contention that both sites 1 and 2 contribute to binding affinity. Whereas substitution of the N-loop (CS1) was sufficient to almost completely swap the affinity of one chemokine to that of the other, substitution of the N-terminus (CS2) also changed the affinity of each chemokine to be closer to that of the other. Importantly, the affinity contributions of these two regions were not simply additive, indicating that the interactions of one region influence those of the other. Our conclusion that site 2 contributes to chemokine-receptor binding is consistent with a study of CCR1-CCR2 chimeric receptors in which regions other than the receptor N-terminus were found to be required for high affinity binding of the CCR1 ligand CCL3/MIP-1α (48).

The CCL7/CCL2 chimeras also provided insights into the roles of chemokine structural regions in receptor activation. Our data indicate that both the N-terminal region and the N-loop contribute to the higher efficacy of CCR1 activation (e.g. E_{max} in the proximal βArr assay) by the full agonist CCL7 compared to the partial agonist CCL2. The contribution of the N-terminal region (CS2) is expected for the two-site, two-step model. However, the contribution of the N-loop (CS1) again suggests interdependence of the site 1 and site 2 interactions, possibly mediated by some of the additional interactions identified by structural modeling (24). These results are consistent with the observation of Pease *et al.* that both the N-terminal region and elements outside of the N-terminal region are required to support CCR1 activation by CCL3 (18).

In summary, the results described here indicate that both sites 1 and 2 contribute to binding interactions but that high affinity receptor binding is not sufficient to give rise to full receptor activation. These results can be rationalized by a fairly simple elaboration of the two-site, two-step model to a "three-step" model (Fig 9), in which: step 1 involves non-specific, low-affinity binding between CS1 and CRS1; step 2 represents specific binding and involves engagement of CS2 with CRS2, possibly accompanied by formation of additional interactions outside the two principal sites; and step 3 involves a conformational change of the chemokine-receptor complex resulting in receptor activation and transmembrane signaling.

The proposed three-step model can be used to understand the interactions of a chemokine receptor with a variety of different types of chemokine ligands (Fig 9). Non-cognate chemokines would participate in step 1 but not in subsequent steps. Cognate chemokine antagonists (or inverse agonists) would participate in steps 1 and 2 but not enable receptor activation. Chemokine agonists would participate in all 3 steps and would shift the equilibrium between the inactive state and the activated state; full agonists would shift this equilibrium strongly towards the activated state, whereas partial agonists would shift it less strongly.

The proposal that site 1 is involved in non-specific binding but that additional interactions are required for specific binding is supported by considerations of binding thermodynamics. Physiological concentrations of chemokines are typically thought to be in the low nanomolar range, although there remains some uncertainty about effective local concentrations, which are expected to be influenced by factors such as oligomerization and glycosaminoglycan binding. Thus, the relatively low affinities of chemokines for the N-terminal regions of their receptors (K_d values in the high nanomolar to low micromolar range) indicates that there will be a relatively low (probably <10%) occupancy of receptor site 1 in the absence of additional interactions. On the other hand, the high affinities of intact receptors for cognate chemokines (K_d values ≤ ~1 nM) will result in high (perhaps >90%) receptor occupancy.

It is also important to consider the kinetics of binding interactions. Previous NMR studies from our lab and others (26-38) have shown that binding of both cognate and non-cognate chemokines to receptor N-terminal peptides is typically fast (dissociation rate constants k_{off} >> 1

s^{-1}), whereas dissociation of cognate chemokines from their receptors is much slower ($k_{off} << 0.1$ s^{-1}), as required for radioligand binding assays. Moreover, conformational transitions from inactive to active states of GPCRs occur with rate constants on the order of ~1 s^{-1} (49). These kinetic considerations suggest that cognate and non-cognate chemokines may bind to and dissociate from site 1 of a receptor many times before a cognate chemokine engages receptor site 2, giving rise to a conformational change and receptor activation. Thus, within the proposed three-step model, step 1 is likely to represent a rapid pre-equilibrium process, whereas step 2 is likely to be the rate-determining step, as indicated by the free energy profiles in Fig 9.

Conclusion – We have proposed a simple three-step model to account for the contributions of site 2 interactions to chemokine-receptor binding affinity and to separate high affinity binding from receptor activation. This model extends the popular two-site, two-step model and may serve as an improved paradigm for interpretation of structure-function and mechanistic experiments. Further elaboration of this model would be possible to incorporate such phenomena as allosteric receptor interactions and ligand-biased receptor activation.

EXPERIMENTAL PROCEDURES

Materials – Dulbecco's Modified Eagle Medium (DMEM) and Hanks's balanced salt solution (HBSS) were purchased from Invitrogen. Blasticidin and Hygromycin B were purchased from InvivoGen (San Diego, CA). Fetal bovine serum was purchased from In Vitro Technologies (Noble Park, VIC, Australia). Polyethyleneimine (PEI) was purchased from Polysciences, Inc. (Warrington, PA). Coelenterazine h was purchased from NanoLight (Pinetop, AZ). Sulfopeptides were synthesised and their concentrations determined as described (50,51). Unless otherwise noted, all the other reagents were purchased from Sigma-Aldrich.

Chemokine Expression and Purification – CCL2 and all chimeras containing the N-terminal region of CCL2 contain the P8A mutation to ensure these proteins are monomeric. The form of CCL15 used in this study is the active, high affinity form CCL15(Δ26), which has the N-terminal sequence HFAAD (52). All chemokines and chimeras were expressed and purified as described (20,46). Briefly, the N-terminal His_6-tagged protein was expressed from BL21 (DE3) *E.coli* in LB media by induction with IPTG. Inclusion bodies containing the fusion (i.e. His_6-tagged) proteins were isolated and dissolved in denaturing buffer and then purified by Ni^{2+}-affinity chromatography. The fusion protein was refolded by rapid dilution, the His_6-tag was removed using human thrombin or TEV protease and the untagged protein (containing the native N-terminus) was further purified by size exclusion chromatography. Purity was evaluated by SDS-PAGE and protein identity was confirmed by MALDI-TOF mass spectrometry.

Fluorescence Anisotropy Assay – Peptides R1A-R1D (Fig 1A) and Fl-R2D (Fig 1A) were prepared by solid phase peptide synthesis and purified by HPLC, as described (41). Samples for fluorescence anisotropy binding assays were prepared in 50 mM MOPS buffer (pH 7.4) using Greiner non-binding, black, flat-bottomed, 96-well microplates and a final volume of 200 μL per well. Direct binding assays were performed using final chemokine concentrations of 31-2000 nM (2-fold increments) and a final concentration of fluorescent sulfopeptide Fl-R2D of 10 nM. Competitive binding assays were performed using invariable final concentrations of the chemokine (100-500 nM; chosen to have ~80 % of the chemokine bound to the probe) and Fl-R2D (10 nM) and with a range of concentrations for the competitor (non-fluorescent sulfopeptides R1A-R1D), serially 2-fold diluted from the highest final concentrations of 100 μM (for R1A), 50 μM (for R1B, R1C) and 10 μM (for R1D). After 5 min, fluorescence anisotropy was measured at 25 °C using a PHERAstar plate reader (BMG Labtech, Ortenberg, Germany) equipped with a fluorescence polarisation module with dedicated excitation and emission wavelengths of 485 and 520 nm respectively. Assays were performed in duplicate, three times independently.

Mammalian Cell Culture – Assays (except the β-arrestin recruitment assay) were performed using Flp-In™ T-REx™ 293 cells (Invitrogen) stably transfected with the plasmid pcDNA5/FRT/TO-His_6-cMyc-CCR1 to express human CCR1 with N-terminal His_6 and cMyc tags. Cells were grown and maintained in full media comprised of Dulbecco's modified eagle medium (DMEM, Gibco) supplemented with 5% (v/v) tetracyclin-free fetal bovine serum (FBS, Gibco), 5 μg/mL blasticidin to maintain selection of cells stably transfected with the tetracyclin repressor gene (tetR) and 200 μg/mL hygromycin B to maintain selection of cells stably transfected with the CCR1 gene. Cells were grown and

maintained at 37 °C in 5% CO_2 in 175 cm^2 flasks and were detached from the flask by washing with versene (PBS/EDTA), followed by incubation in 1% (w/v) trypsin in versene for 5 minutes. Tyrosine sulfation was inhibited 48 hours prior to each experiment by addition of 30 mM sodium chlorate to cell media. Receptor expression was induced 24 hours prior to each experiment by addition of 10 μg/mL tetracycline to cell media.

Membrane Preparation – Cell membranes were prepared by detaching the cells from the flasks, centrifugation at 1500 g for 3 min and resuspension in ice-cold 50 mM MOPS buffer containing 5 mM $MgCl_2$ and 0.1% 3-[(3-cholamidopropyl)-dimethylammonio]-1-propanesulfonic acid (CHAPS), pH 7.4. The lysates were homogenized by sonication and centrifuged at low speed for 5 min. Membrane and cytosolic fractions were separated by centrifugation at 40,000 rcf for 30 min at 4 °C. The pellet containing membranes was resuspended in MOPS buffer containing 5 mM $MgCl_2$ and 0.1% CHAPS, pH 7.4 and stored at -20 °C. Protein concentrations were measured using a BCA protein determination assay (53).

Radioligand binding assays – Competitive binding assays were performed as described by Zweemer *et al*. (54). Briefly, binding assays were performed in a 100-μL reaction volume containing 50 mM MOPS buffer (pH 7.4), 5 mM $MgCl_2$, 0.1% CHAPS, 10 μg of membranes, variable concentrations of chemokines and 50 pM ^{125}I- CCL3 (PerkinElmer). Nonspecific binding was determined in the presence of 10 μM BX471, a CCR1 antagonist. Samples were incubated for 2 h at 37 °C. Binding was terminated by dilution with ice-cold 50 mM MOPS buffer (pH 7.4) supplemented with 0.05% CHAPS and 0.5 M NaCl, followed by rapid filtration through a 96-well GF/C filter plate precoated with 0.5% PEI using a Filtermate-harvester (Perkin Elmer). Filters were washed 3 times with the same ice-cold wash buffer, dried at 50 °C, and 25 μL of MicroScint-O scintillation cocktail (PerkinElmer) was added to each well. Radioactivity was determined using a MicroBeta^2 LumiJET 2460 Microplate Counter (PerkinElmer).

β-Arrestin Recruitment Assay – Recruitment of β-arrestin-2 to CCR1 was assessed in Flp-In™ T-REx™ 293 cells transiently transfected with CCR1-RLuc8 and β-arrestin-2-YFP as described previously (55). Briefly, CCR1-RLuc8 and β-arrestin-2-YFP were transfected at a receptor:arrestin ratio of 1:4 using PEI at a DNA:PEI ratio of 1:6 (56). After 24 h, cells were re-plated in poly-D-Lysine-coated 96-well white opaque CulturPlates (PerkinElmer) then, 48 h after transfection, cells were rinsed and pre-incubated in Hank's Balanced Saline Solution (HBSS) for 30 min at 37 °C. Coelenterazine h was added to each well (final concentration 5 μM) followed by the addition of receptor ligands 5 min later. Cells were incubated for a further 10 min in the dark at 37 °C. BRET measurements were obtained using a PHERAstar plate reader (BMG Labtech, Ortenberg, Germany) that allows for sequential integration of the signals detected at 475 ± 30 and 535 ± 30 nm, using filters with the appropriate band pass. Data are presented as a ligand-induced BRET ratio (baseline-corrected by subtracting the BRET ratio of vehicle treated cells). All experiments were performed in duplicate and repeated independently at least 3 times.

ERK1/2 phosphorylation – Phosphorylation of ERK1/2 was measured using the AlphaScreen® SureFire® p-ERK 1/2 (Thr202/Tyr204) Assay Kit (PerkinElmer, TGR biosciences) following the manufacturer's instructions. Briefly, 4 x10^5 cells/well were seeded in a poly-D-Lysine-coated plate in full media containing 10 μg/mL tetracycline and serum-starved overnight. Initial time-course experiments determined that peak levels of ERK 1/2 phosphorylation were achieved 5 minutes after the addition of chemokines. Therefore, for all concentration-response experiments, cells were stimulated with chemokine for 5 minutes at 37 °C. 10 % v/v FBS was used as a positive control. The reaction was terminated by removal of the media and addition of *SureFire* lysis buffer (100 μL). Cell lysis was assisted by shaking the plates at 600 rpm for 5 minutes. 5 μL of lysate was transferred to a white 384-well Proxiplate™ followed by the addition of 8 μL of *SureFire* AlphaScreen Detection Mix (240:1440:7:7 v/v dilution of *SureFire* Activation Buffer: *SureFire* Reaction Buffer: AlphaScreen Acceptor Beads: AlphaScreen Donor Beads). The plate was incubated in the dark for 1.5 h at 37 °C and the AlphaScreen signal was read on an *Envision*® plate reader (PerkinElmer). Data were normalized to the signal in the absence of chemokine (0 % response) and in the presence of 10 % v/v FBS (100 % response). All experiments were performed in duplicate and repeated independently at least 3 times.

Inhibition of forskolin-induced cAMP production – Cells were plated in a Petri dish

(about 2.5 x 10^6 cells per dish) and allowed to grow overnight in full media at 37 °C, 5 % CO_2. The following day, cells were transfected with a CAMYEL cAMP BRET biosensor (56). Transient transfection was performed using PEI at a DNA:PEI ratio of 1:6. After 24 h, cells were re-plated in poly-D-Lysine-coated 96-well white opaque CulturPlates (PerkinElmer). 48h after transfection cells were rinsed and pre-incubated in Hank's Balanced Saline Solution (HBSS) for 30 min at 37 °C. Cells were then incubated with the RLuc substrate coelenterazine h (final concentration 5 µM) for 5 min, followed by a further 5 min incubation with various concentrations of chemokine. Forskolin was then added for an additional 5 min to a final concentration of 10 µM. BRET measurements were obtained using a PHERAstar plate reader (BMG Labtech, Ortenberg, Germany) that allows for sequential integration of the signals detected at 475 ± 30 and 535 ± 30 nm, using filters with the appropriate band pass. BRET ratio was calculated as the ratio of YFP to RLuc signals, and data are expressed as the percentage of the forskolin-induced signal.

G protein activation assay – Cells were plated in a Petri dish (~2.5 x 10^6 cells per dish) and allowed to grow in full media at 37 °C in 5 % CO_2 overnight. The following day, cells were transfected in full media using DNA ratios of 2:1:1:1 for $G_{\alpha i}$: G_β-Venus(C-terminus):G_γ-Venus(N-terminus): masGRK3-ct-Rluc (57) and a 1:6 total DNA to PEI ratio. Cells were allowed to grow in transfection media mix for 24 hours at 37 °C, 5 % CO_2. Cells were then replated in a poly-D-lysine-coated 96-well white-bottom Culturplate in full media containing 10 µg/mL tetracycline and allowed to grow for another 24 hours. Cells were then washed once with 100 µL of HBSS and incubated in fresh HBSS for ~30 min at 37 °C. Cells were stimulated in HBSS to a total volume of 100 µL per well. The Rluc substrate coelenterazine h was added to each well (final concentration of 5 µM) and cells were incubated for 5 minutes at 37 °C. After 5 minutes, cells were stimulated with chemokines and incubated for a further 10 minutes at 37 °C. Venus and Rluc emission signals (535 and 475 nm respectively) were measured using a PHERAstar plate reader and the ratio of Venus:Rluc was used to quantify relative levels of trimeric G protein dissociation in each well. Data are presented as a ligand-induced BRET ratio (baseline-corrected by subtracting the BRET ratio of vehicle treated cells). All experiments were performed in duplicate and at least three times independently.

Data analysis and Statistics – All data points represent the mean and error bars represent the standard error of the mean (SEM) of at least three independent experiments. Data were analyzed using Prism 6.0 (GraphPad Software Inc., San Diego, CA).

Direct fluorescence anisotropy binding data were fitted with a non-linear 1:1 binding equilibrium model described by the equation:

$$Y = Y_i + (Y_f - Y_i) \times \left(\frac{1}{2P_t}\right)\left[(P_t + L_t + K_d) - \sqrt{((P_t + L_t + K_d)^2 - 4P_tL_t)}\right] \quad \text{(Equation 1)}$$

in which: Y is the observed anisotropy; Y_i and Y_f are the initial and final anisotropy, respectively; P_t is the total concentration of Fl-R2D; L_t is the total concentration of the chemokine; and K_d is the fitted equilibrium dissociation constant.

Competitive fluorescence anisotropy binding data were fitted with the non-linear 1:1 competitive displacement equation derived by Huff et al. (58), in which the concentration of the non-fluorescent peptide was the independent variable while the dependent variable was the observed anisotropy. Fixed input parameters were: the total concentrations of Fl-R2D and chemokine; the final anisotropy value which corresponds to the anisotropy of free Fl-R2D; and the affinity between Fl-R2D and chemokine (K_d value obtained from the direct binding assay). The fitted parameters were the initial anisotropy and the log(K_d) between the competitor and the chemokine.

For radioligand binding, the concentration of agonist that inhibited half of the ^{125}I-CCL3 binding (IC_{50}) was determined using the equation:

$$Y = \frac{Bottom + (top - bottom)}{1 + 10^{(X - logIC_{50})n_H}} \quad \text{(Equation 2)}$$

in which: Y denotes the percentage specific binding; *top* and *bottom* denote the maximal and minimal asymptotes, respectively, of the concentration–response curve; IC_{50} denotes the X-value when the response is midway between Bottom and Top; and n_H denotes the Hill slope factor.

All data from concentration-response signaling assays were normalized as outlined above and fitted to the equation:

$$Y = bottom + \frac{top - bottom}{1 + 10^{(\log EC_{50} - \log[A])}} \quad \text{(Equation 3)}$$

in which: *top* and *bottom* represent the maximal and minimal asymptotes of the concentration–response curve; [A] is the molar concentration of agonist; and EC_{50} is the molar concentration of

agonist required to give a response half way between *bottom* and *top*.

All statistical comparisons were performed using (negative) logarithmic parameters (pK_d, pIC_{50} or pEC_{50}) as distributions of these parameters are approximately Gaussian (59). Multiple T test comparison with Holm-Sidak correction or one way ANOVA were used as stated in Figure Legends. Significance is indicated as * for $p< 0.05$, ** for $p<0.01$ and *** for $p < 0.001$.

Acknowledgements: We thank Ann Stewart and Herman Lim for assistance with cell culture experiments and Simon Foster for critical reading of the manuscript.

Conflict of interest: The authors declare they have no conflict of interest with the content of this manuscript.

Author contributions: JS performed experiments and conducted data analyses; ZH prepared chimeric chemokines; JRL and MC designed and supervised cell-based assays; XL prepared peptide; RJP supervised peptide design and preparation; MJS supervised peptide binding experiments and project strategy; JS and MJS drafted the manuscript and all authors read and critically reviewed the manuscript.

References

1. Moser, B., Wolf, M., Walz, A., and Loetscher, P. (2004) Chemokines: multiple levels of leukocyte migration control. *Trends Immunol.* **25**, 75-84
2. Baggiolini, M. (2001) Chemokines in pathology and medicine. *J. Intern. Med.* **250**, 91-104
3. Gao, J. L., Kuhns, D. B., Tiffany, H. L., McDermott, D., Li, X., Francke, U., and Murphy, P. M. (1993) Structure and functional expression of the human macrophage inflammatory protein 1 alpha/RANTES receptor. *J. Exp. Med.* **177**, 1421-1427
4. Mantovani, A., Bonecchi, R., and Locati, M. (2006) Tuning inflammation and immunity by chemokine sequestration: decoys and more. *Nature reviews. Immunology* **6**, 907-918
5. Stone, M. J., Hayward, J. A., Huang, C., Z, E. H., and Sanchez, J. (2017) Mechanisms of Regulation of the Chemokine-Receptor Network. *Int. J. Mol. Sci.* **18**
6. Tak, P. P., Balanescu, A., Tseluyko, V., Bojin, S., Drescher, E., Dairaghi, D., Miao, S., Marchesin, V., Jaen, J., Schall, T. J., and Bekker, P. (2013) Chemokine receptor CCR1 antagonist CCX354-C treatment for rheumatoid arthritis: CARAT-2, a randomised, placebo controlled clinical trial. *Ann. Rheum. Dis.* **72**, 337-344
7. Trebst, C., Sorensen, T. L., Kivisakk, P., Cathcart, M. K., Hesselgesser, J., Horuk, R., Sellebjerg, F., Lassmann, H., and Ransohoff, R. M. (2001) $CCR1^+/CCR5^+$ mononuclear phagocytes accumulate in the central nervous system of patients with multiple sclerosis. *Am. J. Pathol.* **159**, 1701-1710
8. Karash, A. R., and Gilchrist, A. (2011) Therapeutic potential of CCR1 antagonists for multiple myeloma. *Future Med. Chem.* **3**, 1889-1908
9. Vallet, S., and Anderson, K. C. (2011) CCR1 as a target for multiple myeloma. *Expert Opin. Ther. Targets* **15**, 1037-1047
10. Horuk, R., Clayberger, C., Krensky, A. M., Wang, Z., Grone, H. J., Weber, C., Weber, K. S., Nelson, P. J., May, K., Rosser, M., Dunning, L., Liang, M., Buckman, B., Ghannam, A., Ng, H. P., Islam, I., Bauman, J. G., Wei, G. P., Monahan, S., Xu, W., Snider, R. M., Morrissey, M. M., Hesselgesser, J., and Perez, H. D. (2001) A non-peptide functional antagonist of the CCR1 chemokine receptor is effective in rat heart transplant rejection. *J. Biol. Chem.* **276**, 4199-4204
11. Ribeiro, S., and Horuk, R. (2005) The clinical potential of chemokine receptor antagonists. *Pharmacol. Ther.* **107**, 44-58
12. Hoshino, A., Iimura, T., Ueha, S., Hanada, S., Maruoka, Y., Mayahara, M., Suzuki, K., Imai, T., Ito, M., Manome, Y., Yasuhara, M., Kirino, T., Yamaguchi, A., Matsushima, K., and Yamamoto, K. (2010) Deficiency of chemokine receptor CCR1 causes osteopenia due to impaired functions of osteoclasts and osteoblasts. *J. Biol. Chem.* **285**, 28826-28837
13. Ninichuk, V., and Anders, H. J. (2005) Chemokine receptor CCR1: a new target for progressive kidney disease. *Am. J. Nephrol.* **25**, 365-372
14. Gladue, R. P., Zwillich, S. H., Clucas, A. T., and Brown, M. F. (2004) CCR1 antagonists for the treatment of autoimmune diseases. *Curr. Opin. Investig. Drugs* **5**, 499-504
15. Crump, M. P., Gong, J. H., Loetscher, P., Rajarathnam, K., Amara, A., Arenzana-Seisdedos, F., Virelizier, J. L., Baggiolini, M., Sykes, B. D., and Clark-Lewis, I. (1997) Solution structure and basis for functional activity of stromal cell-derived factor-1; dissociation of CXCR4 activation from binding and inhibition of HIV-1. *EMBO J.* **16**, 6996-7007
16. Qin, L., Kufareva, I., Holden, L. G., Wang, C., Zheng, Y., Zhao, C., Fenalti, G., Wu, H., Han, G. W., Cherezov, V., Abagyan, R., Stevens, R. C., and Handel, T. M. (2015) Structural biology. Crystal structure of the chemokine receptor CXCR4 in complex with a viral chemokine. *Science* **347**, 1117-1122

17. Burg, J. S., Ingram, J. R., Venkatakrishnan, A. J., Jude, K. M., Dukkipati, A., Feinberg, E. N., Angelini, A., Waghray, D., Dror, R. O., Ploegh, H. L., and Garcia, K. C. (2015) Structural biology. Structural basis for chemokine recognition and activation of a viral G protein-coupled receptor. *Science* **347**, 1113-1117
18. Pease, J. E., Wang, J., Ponath, P. D., and Murphy, P. M. (1998) The N-terminal extracellular segments of the chemokine receptors CCR1 and CCR3 are determinants for MIP-1alpha and eotaxin binding, respectively, but a second domain is essential for efficient receptor activation. *J. Biol. Chem.* **273**, 19972-19976
19. Mayer, M. R., and Stone, M. J. (2001) Identification of receptor binding and activation determinants in the N-terminal and N-loop regions of the CC chemokine eotaxin. *J. Biol. Chem.* **276**, 13911-13916
20. Huma, Z. E., Sanchez, J., Lim, H. D., Bridgford, J. L., Huang, C., Parker, B. J., Pazhamalil, J. G., Porebski, B. T., Pfleger, K. D. G., Lane, J. R., Canals, M., and Stone, M. J. (2017) Key determinants of selective binding and activation by the monocyte chemoattractant proteins at the chemokine receptor CCR2. *Sci. Signal.* **10**
21. Xanthou, G., Williams, T. J., and Pease, J. E. (2003) Molecular characterization of the chemokine receptor CXCR3: evidence for the involvement of distinct extracellular domains in a multi-step model of ligand binding and receptor activation. *Eur. J. Immunol.* **33**, 2927-2936
22. Rajagopal, S., Bassoni, D. L., Campbell, J. J., Gerard, N. P., Gerard, C., and Wehrman, T. S. (2013) Biased agonism as a mechanism for differential signaling by chemokine receptors. *J. Biol. Chem.* **288**, 35039-35048
23. Corbisier, J., Gales, C., Huszagh, A., Parmentier, M., and Springael, J. Y. (2015) Biased signaling at chemokine receptors. *J. Biol. Chem.* **290**, 9542-9554
24. Ziarek, J. J., Kleist, A. B., London, N., Raveh, B., Montpas, N., Bonneterre, J., St-Onge, G., DiCosmo-Ponticello, C. J., Koplinski, C. A., Roy, I., Stephens, B., Thelen, S., Veldkamp, C. T., Coffman, F. D., Cohen, M. C., Dwinell, M. B., Thelen, M., Peterson, F. C., Heveker, N., and Volkman, B. F. (2017) Structural basis for chemokine recognition by a G protein-coupled receptor and implications for receptor activation. *Sci. Signal.* **10**
25. Kleist, A. B., Getschman, A. E., Ziarek, J. J., Nevins, A. M., Gauthier, P. A., Chevigne, A., Szpakowska, M., and Volkman, B. F. (2016) New paradigms in chemokine receptor signal transduction: Moving beyond the two-site model. *Biochem. Pharmacol.* **114**, 53-68
26. Simpson, L. S., Zhu, J. Z., Widlanski, T. S., and Stone, M. J. (2009) Regulation of chemokine recognition by site-specific tyrosine sulfation of receptor peptides. *Chem. Biol.* **16**, 153-161
27. Zhu, J. Z., Millard, C. J., Ludeman, J. P., Simpson, L. S., Clayton, D. J., Payne, R. J., Widlanski, T. S., and Stone, M. J. (2011) Tyrosine Sulfation Influences the Chemokine Binding Selectivity of Peptides Derived from Chemokine Receptor CCR3. *Biochemistry* **50**, 1524-1534
28. Schnur, E., Kessler, N., Zherdev, Y., Noah, E., Scherf, T., Ding, F. X., Rabinovich, S., Arshava, B., Kurbatska, V., Leonciks, A., Tsimanis, A., Rosen, O., Naider, F., and Anglister, J. (2013) NMR mapping of RANTES surfaces interacting with CCR5 using linked extracellular domains. *FEBS J.* **280**, 2068-2084
29. Tan, J. H. Y., Ludeman, J. P., Wedderburn, J., Canals, M., Hall, P., Butler, S. J., Taleski, D., Christopoulos, A., Hickey, M. J., Payne, R. J., and Stone, M. J. (2013) Tyrosine sulfation of chemokine receptor CCR2 enhances interactions with both monomeric and dimeric forms of the chemokine monocyte chemoattractant protein-1 (MCP-1). *J. Biol. Chem.* **289**, 13362-13362
30. Veldkamp, C. T., Seibert, C., Peterson, F. C., Sakmar, T. P., and Volkman, B. F. (2006) Recognition of a CXCR4 sulfotyrosine by the chemokine stromal cell-derived factor-1alpha (SDF-1alpha/CXCL12). *J. Mol. Biol.* **359**, 1400-1409
31. Veldkamp, C. T., Seibert, C., Peterson, F. C., De la Cruz, N. B., Haugner, J. C., 3rd, Basnet, H., Sakmar, T. P., and Volkman, B. F. (2008) Structural basis of CXCR4 sulfotyrosine recognition by the chemokine SDF-1/CXCL12. *Sci. Signal.* **1**, ra4
32. Millard, C. J., Ludeman, J. P., Canals, M., Bridgford, J. L., Hinds, M. G., Clayton, D. J., Christopoulos, A., Payne, R. J., and Stone, M. J. (2014) Structural Basis of Receptor Sulfotyrosine Recognition by a CC Chemokine: The N-Terminal Region of CCR3 Bound to CCL11/Eotaxin-1. *Structure* **22**, 1571-1581
33. Duma, L., Haussinger, D., Rogowski, M., Lusso, P., and Grzesiek, S. (2007) Recognition of RANTES by extracellular parts of the CCR5 receptor. *J. Mol. Biol.* **365**, 1063-1075
34. Chaudhuri, A., Basu, P., Haldar, S., Kombrabail, M., Krishnamoorthy, G., Rajarathnam, K., and Chattopadhyay, A. (2013) Organization and dynamics of the N-terminal domain of chemokine receptor CXCR1 in reverse micelles: effect of graded hydration. *J. Phys. Chem. B* **117**, 1225-1233
35. Fernando, H., Nagle, G. T., and Rajarathnam, K. (2007) Thermodynamic characterization of interleukin-8 monomer binding to CXCR1 receptor N-terminal domain. *FEBS J.* **274**, 241-251
36. Haldar, S., Raghuraman, H., Namani, T., Rajarathnam, K., and Chattopadhyay, A.

Membrane interaction of the N-terminal domain of chemokine receptor CXCR1. *Biochim. Biophys. Acta* **1798**, 1056-1061
37. Rajarathnam, K., Prado, G. N., Fernando, H., Clark-Lewis, I., and Navarro, J. (2006) Probing receptor binding activity of interleukin-8 dimer using a disulfide trap. *Biochemistry* **45**, 7882-7888
38. Stone, M. J., and Payne, R. J. (2015) Homogeneous Sulfopeptides and Sulfoproteins: Synthetic Approaches and Applications To Characterize the Effects of Tyrosine Sulfation on Biochemical Function. *Acc. Chem. Res.* **48**, 2251-2261
39. Liu, J., Louie, S., Hsu, W., Yu, K. M., Nicholas, H. B., Jr., and Rosenquist, G. L. (2008) Tyrosine sulfation is prevalent in human chemokine receptors important in lung disease. *Am. J. Respir. Cell Mol. Biol.* **38**, 738-743
40. Choe, H., Moore, M. J., Owens, C. M., Wright, P. L., Vasilieva, N., Li, W., Singh, A. P., Shakri, R., Chitnis, C. E., and Farzan, M. (2005) Sulphated tyrosines mediate association of chemokines and Plasmodium vivax Duffy binding protein with the Duffy antigen/receptor for chemokines (DARC). *Mol. Microbiol.* **55**, 1413-1422
41. Ludeman, J. P., Nazari-Robati, M., Wilkinson, B. L., Huang, C., Payne, R. J., and Stone, M. J. (2015) Phosphate modulates receptor sulfotyrosine recognition by the chemokine monocyte chemoattractant protein-1 (MCP-1/CCL2). *Org. Biomol. Chem.* **13**, 2162-2169
42. Chou, C. C., Fine, J. S., Pugliese-Sivo, C., Gonsiorek, W., Davies, L., Deno, G., Petro, M., Schwarz, M., Zavodny, P. J., and Hipkin, R. W. (2002) Pharmacological characterization of the chemokine receptor, hCCR1 in a stable transfectant and differentiated HL-60 cells: antagonism of hCCR1 activation by MIP-1beta. *Brit. J. Pharmacol.* **137**, 663-675
43. Combadiere, C., Ahuja, S. K., Van Damme, J., Tiffany, H. L., Gao, J. L., and Murphy, P. M. (1995) Monocyte chemoattractant protein-3 is a functional ligand for CC chemokine receptors 1 and 2B. *J. Biol. Chem.* **270**, 29671-29675
44. Coulin, F., Power, C. A., Alouani, S., Peitsch, M. C., Schroeder, J. M., Moshizuki, M., Clark-Lewis, I., and Wells, T. N. (1997) Characterisation of macrophage inflammatory protein-5/human CC cytokine-2, a member of the macrophage-inflammatory-protein family of chemokines. *Eur. J. Biochem.* **248**, 507-515
45. Schmidt, P. M., Sparrow, L. G., Attwood, R. M., Xiao, X., Adams, T. E., and McKimm-Breschkin, J. L. (2012) Taking down the FLAG! How insect cell expression challenges an established tag-system. *PloS one* **7**, e37779
46. Tan, J. H. Y., Canals, M., Ludeman, J. P., Wedderburn, J., Boston, C., Butler, S. J., Carrick, A. M., Parody, T. R., Taleski, D., Christopoulos, A., Payne, R. J., and Stone, M. J. (2012) Design and receptor interactions of obligate dimeric mutant of chemokine monocyte chemoattractant protein-1 (MCP-1). *J. Biol. Chem.* **287**, 14692-14702
47. Paavola, C. D., Hemmerich, S., Grunberger, D., Polsky, I., Bloom, A., Freedman, R., Mulkins, M., Bhakta, S., McCarley, D., Wiesent, L., Wong, B., Jarnagin, K., and Handel, T. M. (1998) Monomeric monocyte chemoattractant protein-1 (MCP-1) binds and activates the MCP-1 receptor CCR2B. *J. Biol. Chem.* **273**, 33157-33165
48. Monteclaro, F. S., and Charo, I. F. (1996) The amino-terminal extracellular domain of the MCP-1 receptor, but not the RANTES/MIP-1alpha receptor, confers chemokine selectivity. Evidence for a two-step mechanism for MCP-1 receptor activation. *J. Biol. Chem.* **271**, 19084-19092
49. Vilardaga, J. P. (2010) Theme and variations on kinetics of GPCR activation/deactivation. *J Recept. Signal Transduct. Res.* **30**, 304-312
50. Taleski, D., Butler, S. J., Stone, M. J., and Payne, R. J. (2011) Divergent and Site-Selective Solid-Phase Synthesis of Sulfopeptides. *Chem. Asian J.* **6**, 1316-1320
51. Zhu, J. Z., Millard, C. J., Ludeman, J. P., Simpson, L. S., Clayton, D. J., Payne, R. J., Widlanski, T. S., and Stone, M. J. (2011) Tyrosine sulfation influences the chemokine binding selectivity of peptides derived from chemokine receptor CCR3. *Biochemistry* **50**, 1524-1534
52. Escher, S. E., Forssmann, U., Frimpong-Boateng, A., Adermann, K., Vakili, J., Sticht, H., and Detheux, M. (2004) Functional analysis of chemically synthesized derivatives of the human CC chemokine CCL15/HCC-2, a high affinity CCR1 ligand. *J Pept Res* **63**, 36-47
53. Smith, P. K., Krohn, R. I., Hermanson, G. T., Mallia, A. K., Gartner, F. H., Provenzano, M. D., Fujimoto, E. K., Goeke, N. M., Olson, B. J., and Klenk, D. C. (1985) Measurement of protein using bicinchoninic acid. *Anal. Biochem.* **150**, 76-85
54. Zweemer, A. J., Nederpelt, I., Vrieling, H., Hafith, S., Doornbos, M. L., de Vries, H., Abt, J., Gross, R., Stamos, D., Saunders, J., Smit, M. J., Ijzerman, A. P., and Heitman, L. H. (2013) Multiple binding sites for small-molecule antagonists at the CC chemokine receptor 2. *Mol. Pharmacol.* **84**, 551-561
55. Ayoub, M. A., Zhang, Y., Kelly, R. S., See, H. B., Johnstone, E. K. M., McCall, E. A., Williams, J. H., Kelly, D. J., and Pfleger, K. D. G. (2015) Functional interaction between angiotensin II receptor type 1 and chemokine (C-C motif) receptor 2 with implications for chronic kidney disease. *PloS one* **10**
56. Scholten, D. J., Canals, M., Wijtmans, M., de Munnik, S., Nguyen, P., Verzijl, D., de Esch, I. J., Vischer, H. F., Smit, M. J., and Leurs, R. (2012) Pharmacological characterization of a small-

molecule agonist for the chemokine receptor CXCR3. *Brit. J. Pharmacol.* **166**, 898-911
57. Hollins, B., Kuravi, S., Digby, G. J., and Lambert, N. A. (2009) The c-terminus of GRK3 indicates rapid dissociation of G protein heterotrimers. *Cell. Signal.* **21**, 1015-1021
58. Huff, S., Matsuka, Y. V., McGavin, M. J., and Ingham, K. C. (1994) Interaction of N-terminal fragments of fibronectin with synthetic and recombinant D motifs from its binding protein on Staphylococcus aureus studied using fluorescence anisotropy. *J. Biol. Chem.* **269**, 15563-15570
59. Christopoulos, A. (1998) Assessing the distribution of parameters in models of ligand-receptor interaction: to log or not to log. *Trends Pharmacol. Sci.* **19**, 351-357

FOOTNOTES

This work was supported by National Health and Medical Research Council Project Grant APP1140874 (MJS, MC, JRL), Australian Research Council Discovery Grant DP130101984 (RJP, MJS), Monash Institute of Pharmaceutical Sciences Large Grant Support Scheme (MC) and Monash University Joint Medicine-Pharmacy grant JMP16-18 (MJS and MC).

The abbreviations used are: βArr, recruitment of β-Arrestin 2; BRET, bioluminescence resonance energy transfer; CCL, CC chemokine ligand; CCR, CC chemokine receptor; CHAPS, 3-((3-cholamidopropyl) dimethylammonio)-1-propanesulfonate; CS, chemokine site; CRS1, chemokine receptor site; DMEM, Dulbecco's Modified Eagle Medium; EC_{50}, 50% maximal effective concentration; EDTA, ethylenediaminetetraacetic acid; ERK1/2, extracellular signal-regulated kinases 1 and 2; FBS, fetal bovine serum; GPCR, G protein-coupled receptor; HCC-2, hemofiltrate CC chemokine 2; HBSS, Hanks's balanced salt solution; HEK, human embryonic kidney; IC_{50}, 50% inhibitory concentration; MALDI-TOF, matrix-assisted laser desorption ionization time-of-flight; MCP, monocyte chemoattractant protein; MIP, macrophage inflammatory protein; MOPS, 3-(N-morpholino)propanesulfonic acid; PBS, phosphate-buffered saline; PEI, polyethyleneimine; RANTES, regulated on activation normal T cell expression and secretion; SDS-PAGE, sodium dodecyl sulfate polyacrylamide gel electrophoresis; SEM, standard error of the mean; tetR, tetracyclin repressor; TM, transmembrane; YFP, yellow fluorescent protein.

TABLE 1. Affinities for binding of CC chemokines to CCR1 N-terminal peptides

Binding constants are reported as pK_d values (-$\log_{10}$ of the K_d; in M) ± S.E. The corresponding K_d values (in μM) are in parentheses. CCL7 in each peptide's data set was used as a reference for statistical analysis.

Chemokine	Competitive Binding pK_d			
	R1A	**R1B**	**R1C**	**R1D**
CCL2	5.1 ± 0.07 (9.1)	5.8 ± 0.03 (1.4)***	6.4 ± 0.04 (0.4)*	6.9 ± 0.05 (0.1)***
CCL5	5.8 ± 0.03 (1.7)***	6.6 ± 0.03 (0.2)***	6.8 ± 0.02 (0.2)*	7.1 ± 0.03 (0.1)**
CCL7	5.3 ± 0.05 (4.7)	6.1 ± 0.03 (0.8)	6.6 ± 0.04 (0.2)	7.3 ± 0.02 (0.1)
CCL8	5.5 ± 0.03 (3.2)	6.2 ± 0.04 (0.6)	7.1 ± 0.01 (0.1)***	7.4 ± 0.04 (0.04)
CCL15	4.6 ± 0.06 (23.9)***	5.1 ± 0.05 (8.8)***	5.4 ± 0.05 (4.3)***	5.6 ± 0.04 (2.3)***
CCL26	5.4 ± 0.06 (4.0)	6.1 ± 0.05 (0.8)	6.4 ± 0.05 (0.4)*	6.8 ± 0.02 (0.1)***

TABLE 2. Affinities for binding of CC chemokines to CCR1. Binding was determined using a radioligand (^{125}I- CCL3) displacement assay with membranes prepared from cells grown in the absence of chlorate or the presence of 30 mM chlorate to inhibit sulfation for 48 h prior to membrane preparation. CCR1 expression was induced by addition of 10 μg/mL tetracycline to the cell media 24 hours prior to membrane preparation. Inhibition constants are reported as pIC_{50} values ($-\log_{10}$ of the IC_{50}; in M) ± S.E. The corresponding IC_{50} values (in nM) are in parentheses. CCL7 was used as a reference for statistical analysis.

Chemokine	**p*IC*$_{50}$ (No chlorate treatment)**	**p*IC*$_{50}$ (Chlorate-treated cells)**
CCL2	7.2 ± 0.1 (57.5)***	7.7 ± 0.1 (19.1)***
CCL5	9.2 ± 0.2 (0.6)	9.7 ± 0.1 (0.2)
CCL7	9.6 ± 0.1 (0.4)	9.8 ± 0.1(0.2)
CCL8	8.7 ± 0.2 (1.8)*	8.7 ± 0.1 (1.9)***
CCL15	10.1 ± 0.2 (0.07)	10.0 ± 0.1 (0.1)
CCL26	no binding	6.3 ± 0.2 (457.1)***

TABLE 3. CCR1 binding and activation parameters for CCL2/CCL7 chimeras

Binding inhibition constants are reported as pIC_{50} values ($-\log_{10}$ of the IC_{50}; in M) ± S.E. Potency values for receptor activation are reported as pEC_{50} values ($-\log_{10}$ of the EC_{50}; in M) ± S.E. The corresponding IC_{50} and EC_{50} values (in nM) are in parentheses. Maximal effects (E_{max}) are reported as normalized values: the maximal response used for normalization was CCL7 (1 μM) for βArr and GPA assays, forskolin (10 μM) for cAMP assay and FBS (10 %) for pERK assay. CCL7 was used as a reference in each assay for statistical analysis. "nd" indicates values that could not be determined from the data.

	CCR1 Binding	**β-Arrestin-2 Assay**		**GPA Assay (α_{i2})**		**cAMP Assay**		**pERK Assay**	
	p*IC*$_{50}$	**p*EC*$_{50}$**	**E$_{max}$**	**p*EC*$_{50}$**	**E$_{max}$**	**p*EC*$_{50}$**	**E$_{max}$**	**p*EC*$_{50}$**	**E$_{max}$**
CCL2	7.2 ± 0.2 (57)***	7.8 ± 0.3 (17)	58.6 ± 8**	<6.5 (>300)	nd	<6.5 (>300)	nd	6.9 ± 0.1 (130)***	24.2 ± 2***
CCL2-722	8.0 ± 0.1 (9.3)***	7.8 ± 0.2 (14)	72.1 ± 6	<6.5 (>300)	nd	6.9 ± 0.2 (277)**	38.4 ± 5	7.6 ± 0.2 (24)*	33.7 ± 2*
CCL2-272	9.0 ± 0.1 (1.0)	7.8 ± 0.1 (16)	70.5 ± 4	<6.5 (>300)	nd	7.3 ± 0.1 (54)	42.5 ± 3	7.7 ± 0.2 (22)	31.4 ± 2**
CCL2-227	7.2 ± 0.1 (63)***	<7.0 (>300)	nd	<6.5 (>300)	nd	<6.5 (>300)	nd	7.0 ± 0.1 (110)***	27.1 ± 2***
CCL2-777	9.8 ± 0.1 (0.2)***	8.3 ± 0.1 (5.6)	107.0 ± 6	7.3 ± 0.1 (45.9)	93.6 ± 4	7.6 ± 0.1 (26)	49.5 ± 3	7.8 ± 0.1 (15)	37.8 ± 2
CCL7	9.0 ± 0.1 (1.0)	8.3 ± 0.1 (5.2)	97.8 ± 5	7.4 ± 0.1 (35.7)	105.5 ± 5	7.9 ± 0.2 (14)	44.2 ± 3	8.2 ± 0.2 (6.0)	43.7 ± 2
CCL7-277	8.1 ± 0.1 (7.2)***	8.2 ± 0.2 (6.7)	76.5 ± 6	<6.5 (>300)	nd	7.5 ± 0.2 (33)	37.9 ± 3	7.2 ± 0.2 (64)***	32.3 ± 3**
CCL7-727	7.8 ± 0.1 (16)***	8.2 ± 0.2 (6.8)	82.6 ± 6	<6.5 (>300)	nd	7.2 ± 0.1 (62)*	39.7 ± 3	7.6 ± 0.1 (24)*	40.5 ± 1
CCL7-772	8.5 ± 0.2 (3.4)*	8.7 ± 0.2 (2.0)	97.4 ± 7	7.6 ± 0.1 (27.1)	90.4 ± 11	7.9 ± 0.1 (14)	50.3 ± 2	8.2 ± 0.1 (6.8)	50.2 ± 2
CCL7-222	7.2 ± 0.1 (61)***	nd	nd	<6.5 (>300)	nd	<6.5 (>300)	nd	6.5 ± 0.1 (350)***	22.1 ± 3***

FIGURE LEGENDS

FIGURE 1. Binding of CC chemokines to CCR1 N-terminal peptides. (A) Sequences of CCR1 peptides R1A-D; sulfated tyrosine residues (sY) are indicated in bold underlined red font whereas non-sulfated tyrosine residues are shown in bold black font. (**B-G**) Competitive binding data and fitted curves (solid lines) for displacement of fluorescent peptide Fl-R2D (sequence Fl-EEVTTFFDsYDsYGAP, in which Fl represents fluorescein and sY represents sulfotyrosine) from **(B)** CCL2, **(C)** CCL5, **(D)** CCL7, **(E)** CCL8, **(F)** CCL15 and **(G)** CCL26 using each of the four CCR1 N-terminal peptides: R1A (blue circles), R1B (red squares), R1C (green triangles) and R1D (purple inverted triangles). For all data points, the concentrations of Fl-R2D and the chemokine were 10 and 100 nM, respectively. Data points represent mean ± SEM of at least three independent experiments performed in duplicate.

FIGURE 2. Binding of CC chemokines to CCR1. The radioligand displacement assay was performed using ^{125}I-CCL3 as a probe and membrane preparations of Flp-In T-REx HEK293 cells expressing His_6-cMyc-CCR1 grown (A) in the absence and (B) in the presence of 30 mM sodium chlorate. Receptor expression was induced 24 hours prior to membrane preparation by addition of 10 μg/mL tet to cell media. For the data shown in panel (B), sulfation was inhibited by treatment of the cells with chlorate for 48 h prior to membrane preparation. Data points represent means ± SEM of at least three independent experiments performed in triplicate.

FIGURE 3. Correlation of chemokines binding affinities of CCR1 and N-terminal peptides. Data points represent the pIC_{50} value for CCR1 (x-axis) and the pK_d values for **(A)** R1A, **(B)** R1B, **(C)** R1C and **(D)** R1D (y-axis) for five chemokines; data were not available for CCL26 as it did not bind detectably to CCR1 at concentrations tested. Data points represent mean ± SEM of at least three independent experiments. For all four graphs the squared correlation coefficient (r^2) is ≤0.16.

FIGURE 4. Design and nomenclature of CCL2/CCL7 chimeras. (A) Structure of CCL7 (PDB ID: 1BO0) showing the three regions swapped in the chimeras. **(B)** Schematic diagrams of the chimeras with regions from CCL2 and CCL7 in blue and red respectively.

FIGURE 5. Binding and activation of CCR1 by CCL2, CCL7 and triple-swap chimeras. (A) Competitive displacement was measured using membrane preparations of His_6-cMyc-CCR1 Flp-In T-REx 293 cells and ^{125}I-CCL3 as a probe. **(B)** β-Arrestin 2 recruitment was measured using parental HEK 293 cells transiently transfected with plasmids encoding CCR1-RLuc8 and β-Arr2-YFP. **(C)** G protein activation was measured using His_6-cMyc-CCR1 Flp-In T-REx 293 cells and $G\alpha_{i2}$. **(D)** cAMP inhibition was measured using His_6-cMyc-CCR1 Flp-In T-REx 293 cells transiently transfected with a BRET-based cAMP biosensor. **(E)** ERK1/2 phosphorylation assay was performed using His_6-cMyc-CCR1 Flp-In T-REx 293 cells and the amount of phosphorylated ERK1/2 was measured by AlphaScreen detection. Data points represent means ± SEM of at least three independent experiments.

FIGURE 6. Binding and activation of CCR1 by β3 swap chimeras. (A) Competitive displacement, **(B)** β-arrestin 2 recruitment, **(C)** G protein activation, **(D)** cAMP inhibition and **(E)** ERK1/2 phosphorylation were measured as described for Fig 5. Data points represent means ± SEM of at least three independent experiments.

FIGURE 7. Binding and activation of CCR1 by N-loop swap chimeras. (A) Competitive displacement, **(B)** β-arrestin 2 recruitment, **(C)** G protein activation, **(D)** cAMP inhibition and **(E)** ERK1/2 phosphorylation were measured as described for Fig 5. Data points represent means ± SEM of at least three independent experiments.

FIGURE 8. Binding and activation of CCR1 by N-terminal swap chimeras. (A) Competitive displacement, **(B)** β-arrestin 2 recruitment, **(C)** G protein activation, **(D)** cAMP inhibition and **(E)**

ERK1/2 phosphorylation were measured as described for Fig 5. Data points represent means ± SEM of at least three independent experiments.

FIGURE 9. Proposed "three-step" model for chemokine receptor binding and activation. (Top) Mechanistic model in which the three steps (left to right) represent: (1) fast association of receptor (R) and ligand (L) via site 1 to give low affinity, non-specific complex (RL^{NS}); (2) slow formation of site 2 interactions to give a high affinity, specific complex (RL^{Spec}); and (3) a conformational change to the ligand-bound, activated state of the receptor (RL^{Act}). (Bottom) Corresponding, hypothetical free energy profile for an agonist (solid black curve) at a concentration (typically 10-100 nM) intermediate between the K_d values for high affinity receptor binding and low affinity binding at site 1 only. Also shown are the free energy profiles expected for a high affinity antagonist (red curve) a low affinity non-cognate ligand (cyan curve) at a similar concentration. The basal activity of the unliganded receptor is represented by the dashed black curve.

Figure 1. Binding of CC chemokines to CCR1 N-terminal peptides

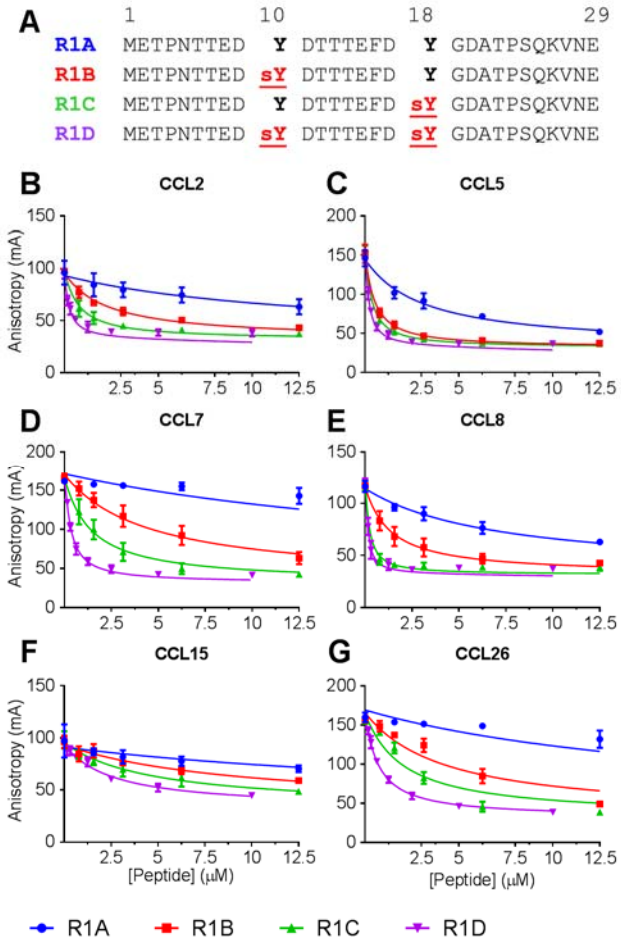

Figure 2. Binding of CC chemokines to CCR1.

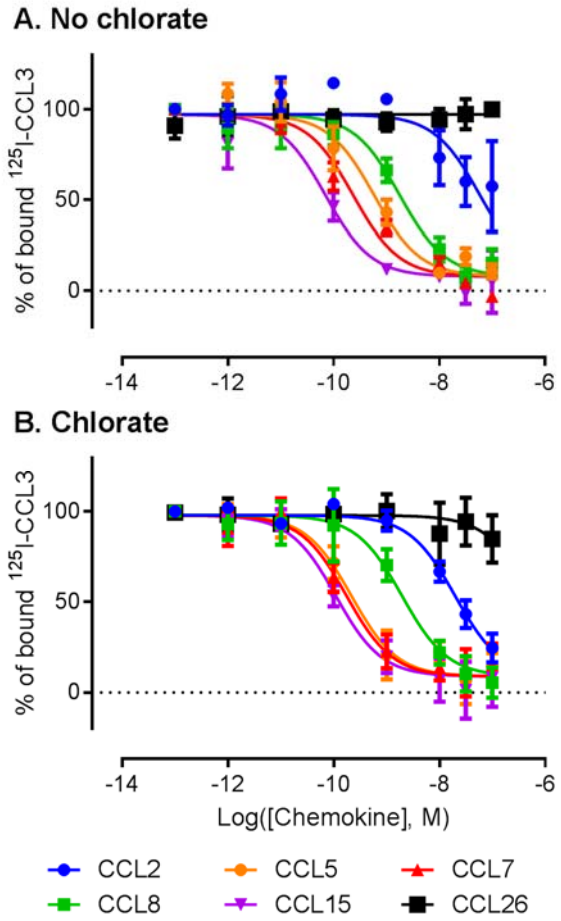

Figure 3. Correlation of chemokine binding affinities of CCR1 and N-terminal peptides.

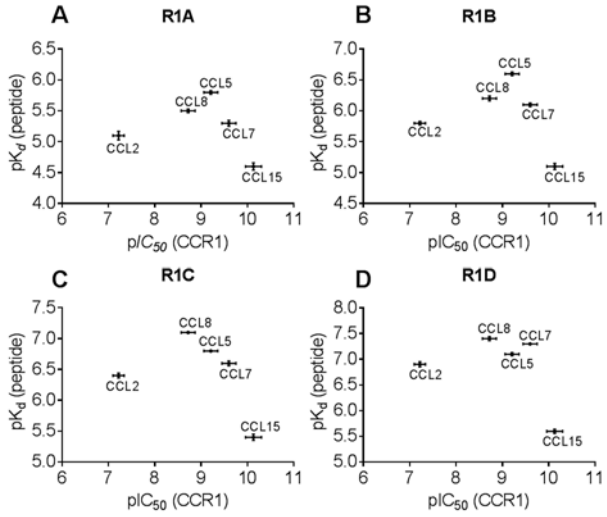

Figure 4. Design and nomenclature of CCL2/CCL7 chimeras

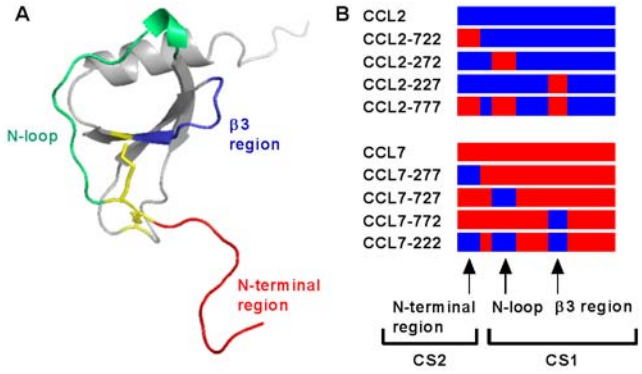

Figure 5. Binding and activation of CCR1 by CCL2, CCL7 and triple-swap chimeras

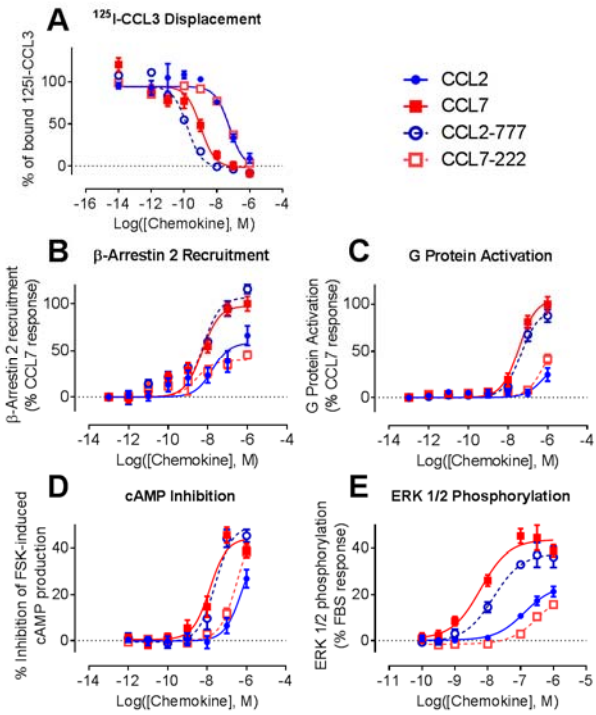

Figure 6. Binding and activation of CCR1 by β3 swap chimeras

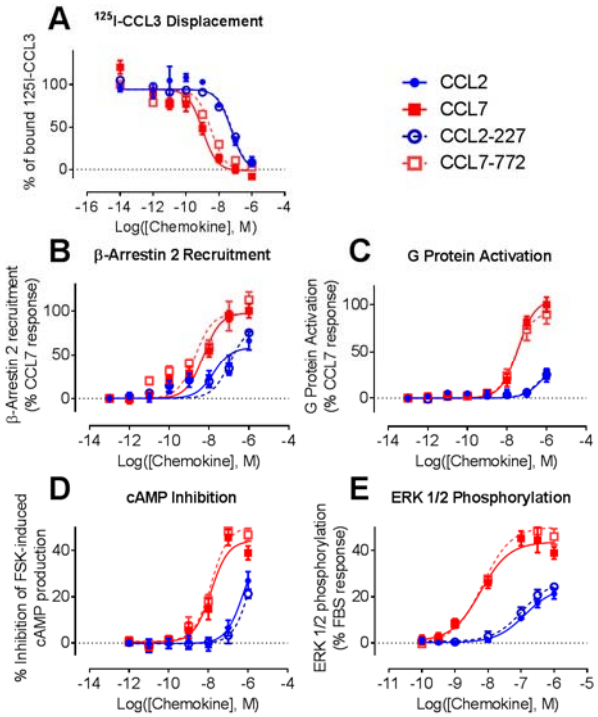

Figure 7. Binding and activation of CCR1 by N-loop swap chimeras

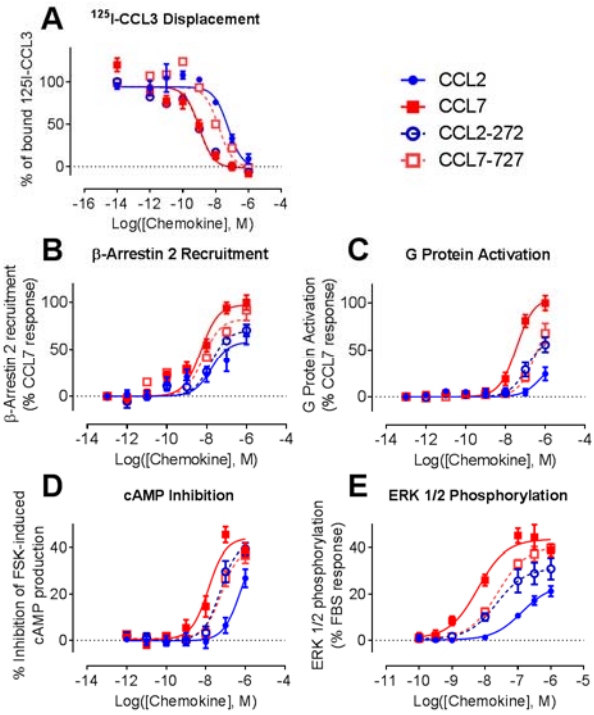

Figure 8. Binding and activation of CCR1 by N-terminal swap chimeras

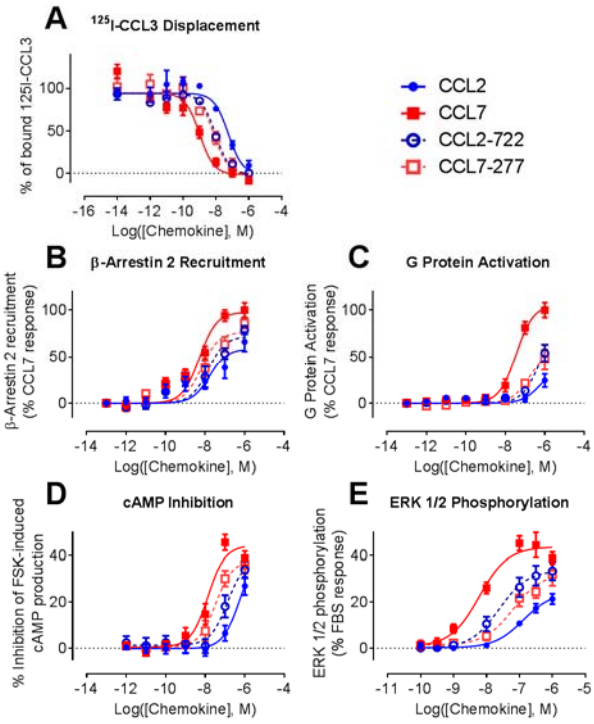

Figure 9. Proposed "three-step" model for chemokine receptor binding and activation.